

A Phase Correction Method in G.O. Designed Dielectric Lens Horn Antenna

Atsushi Kezuka¹, Yoshihide Yamada¹, Yasuhiro Kazama²

¹National Defense Academy

1-10-20, Hashirimizu, Yokosuka-shi, Kanagawa, 239-8686, Japan

²Japan Radio Co., Ltd

5-1-1, Shimorenjaku, Mitaka-shi, Tokyo, 181-8510, Japan

Email: d03003@nda.ac.jp

1. Introduction

TM₀₁ mode horns were mainly employed as a reflector antenna feeds so as to achieve omni-directional coverage around the vertical axis[1][2]. When a shaped beam was designed in the vertical plane, low sidelobe characteristics became important[2]. A dielectric lens horn was introduced. In this paper, accurate radiation characteristics are calculated through FDTD analyses. As for a phase distribution designing, a G.O.(geometrical optics) design is shown insufficient. A method of correcting a lens surface is developed. Then, validity of the method is ensured through FDTD analyses.

2. Design of lens surfaces through a G.O. method

Electrical fields in a conical horn with TM₀₁ mode are radial symmetrical as shown in Fig.1[3]. The electrical field distribution is given by the next expression.

$$E_{r,0}(r) = CJ_1(2.405r/r_0)e^{-jkr^2/Tc} \tag{1}$$

Where, Tc indicates axial horn length. $J_1(\)$ is Bessel function of the first order. The term of exponent indicates a phase variation in the r-direction on an aperture plane. In order to achieve low sidelobe characteristics, aperture fields are tapered by a dielectric lens as given by the next equation.

$$E_{r,1}(r) = CJ_1(2.405r/r_0) \cdot (r_0 - r)/r_0 \tag{2}$$

The term $(r_0 - r)/r_0$ in equation(2) gives low sidelobe characteristics. Equation(2) also indicates that phase delay caused by horn flare is corrected to be uniform.

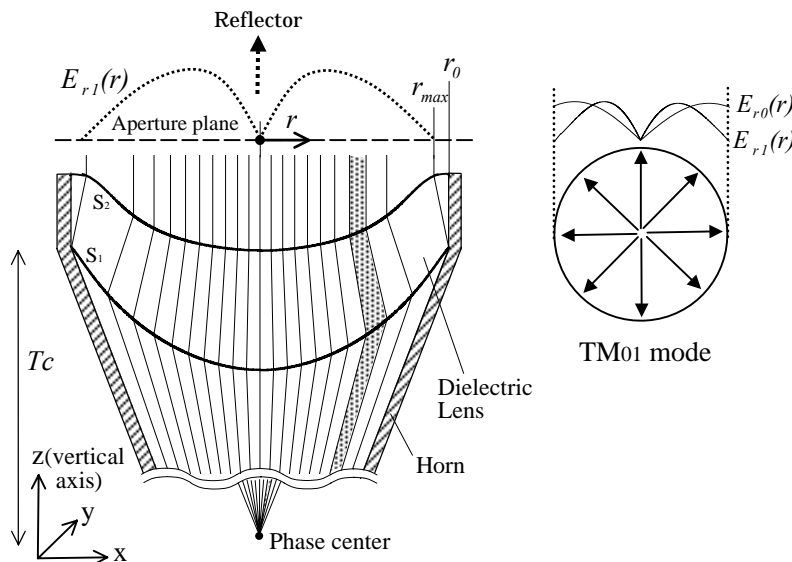


Fig.1 G.O. designed TM₀₁ mode lens horn

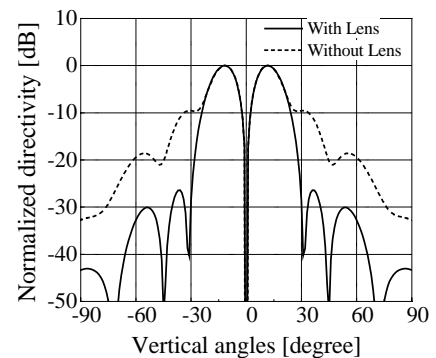


Fig.2 Radiation patterns

Lens curvatures are designed by a G.O.method[4]. The amplitude distribution is achieved by energy conservation condition in ray tubes. Shapes of designed lens curvatures are shown in Fig.1. Here,

design frequency is 25.8GHz and r_0 becomes 26.3mm($2.3\lambda_0$). Polycarbonate is employed as a lens material whose dielectric constant is 2.8. Radiation patterns are obtained through integrating aperture fields. Calculated results are shown in Fig.2. The solid line shows radiation pattern of a dielectric lens horn. The dotted line shows radiation pattern of a horn without a dielectric lens. Here, aperture size for with and without lens are adequately selected in order to achieve the same beam width. It is shown that low sidelobe levels are achieved by a dielectric lens insertion. Reflection and other effects that disturb aperture fields are not accounted in the calculation. So, this radiation pattern in Fig.2 and distributions of equation(2) become design objectives.

3. FDTD analyses

Realizations of a design objective are examined through FDTD. In analyses, cell dimensions of $\Delta x = \Delta y = 0.448\text{mm}$, and $\Delta z = 0.45\text{mm}(\lambda_{gr}/15)$ are employed. Cell number becomes $179 \times 179 \times 225$. Matching layers are attached to lens surfaces in order to reduce reflections on lens surfaces. A dielectric constants of matching layers is $\sqrt{\epsilon_r}$ and thickness is $\lambda_0 / 4\sqrt{\epsilon_r}$.

Calculated radiation patterns of the designed antenna are shown in Fig.3. It is shown that sidelobe pattern changes in accordance with the frequency change become small by the effect of matching layers. When comparing calculated results and the design objective, they don't agree any more. Side lobe levels become higher than that of the design objective. Amplitude and phase distributions on apertures of the antenna are shown in Fig.4(a) and Fig.4(b), respectively. In Fig.4(a), amplitude is sufficiently agree with the design objective given by equation(2). In Fig.4(a), it is observed that the amplitude distribution is successfully designed by a dielectric lens insertion. As for phase distributions in Fig.4(b), calculated phase distributions and design objectives don't agree anymore. The phases calculated through FDTD get behind the design objective. Phase delays are increasing toward the edge of a dielectric lens. The phase delay of 120 degree is occurred at the edge.

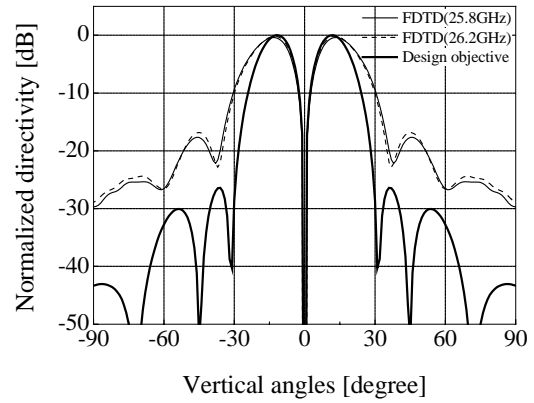
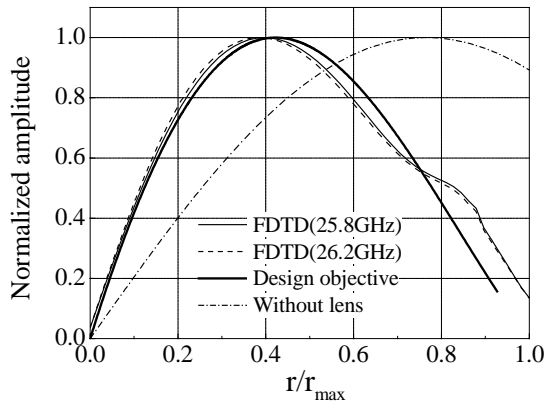
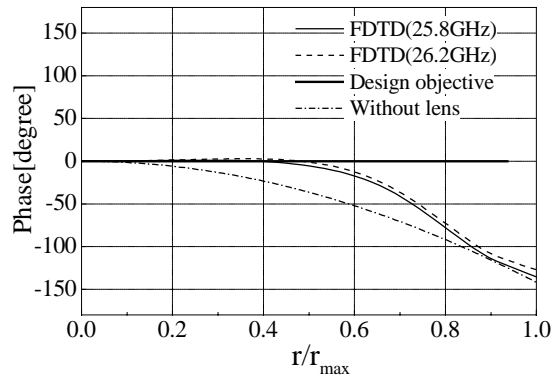


Fig.3 Radiation patterns through FDTD



(a) Amplitude distributions



(b) Phase distributions

Fig.4 Aperture fields calculated through FDTD

4. Phase correction by a dielectric lens curvature design

4.1 Designing Equation

Concept of a phase correction is shown in Fig.5. Original lens surfaces are indicated by S_1 and S_2 . In order to achieve phase correction, S_2 is moved to S'_2 . A ray path of $P_1 \Rightarrow P_2 \Rightarrow P_a$ is supposed to be changed to a path of $P_1 \Rightarrow P'_2 \Rightarrow P_a$. When the phase correction value $\phi(r/r_{max})$ is converted to the path length value $l(r/r_{max})$ of equation(3), a path length relation is expressed by equation(4). The ray direction of P'_2 to P_a should be ensured after the curvature P'_2 is determined.

4.2 Designed Result

The phase correction function $\phi(r/r_{max})$ is determined through calculation results shown in Fig.4(b). $\phi(r/r_{max})$ is shown by the solid line in Fig.6. After applying $\phi(r/r_{max})$ to equation(4), a corrected lens surface S'_2 is achieved as shown in Fig.7. Lens thickness is reduced in the modified lens surface(S'_2).

Ray tracing method is newly applied to the corrected lens surface. The phase distributions on an aperture through a ray tracing method is shown by the dotted line in Fig.6. The result shows that objective phases are accomplished in the aperture. So, the ray direction of P'_2 to P_a in Fig.5 is nearly achieved in the case of the corrected surface S'_2 . Traced rays are shown in Fig.7. Rays refracted by the lens surface S'_2 are no more parallel and an amplitude distribution may chaged slightly from the design objective.

4.3 Calculated Results by FDTD

Amplitude and phase distributions calculated through FDTD are show in Fig.8(a) and Fig.8(b), respectively. In calculations of FDTD, matching layers are attached to dielectric lens surfaces. In Fig.8(a), the broken line shows the amplitude distribution through a ray-tracing method for corrected surface. Amplitude distributions calculated by ray tracing keeps almost the same shape as the design objective. Moreover, amplitude distributions calculated through FDTD is similarly the same as the design objectives. It is shown that amplitude deviations are small in this correction method. As for phase distributions, phases calculated through FDTD are almost uniform. Maximum phase difference of less than 25degree is accomplished in an aperture. Validity of the phase correction method is conceived. Radiation patterns calculated through FDTD are shown in Fig.9. Sidelobe levels decrease more than 10dB. Effectiveness of a phase correction is ensured.

$$l(r/r_{max}) = \phi(r/r_{max}) \cdot \frac{\lambda}{2\pi} \quad (3)$$

$$n\sqrt{(r_f - r_b)^2 + (z_f - z_b)^2} + (z_{ap} - z_b) = n\sqrt{(r_f - r'_b)^2 + (z_f - z'_b)^2} + \sqrt{(r'_b - r_{ap})^2 + (z'_b - z_{ap})^2} + l(r_b/r_{max}) \quad (4)$$

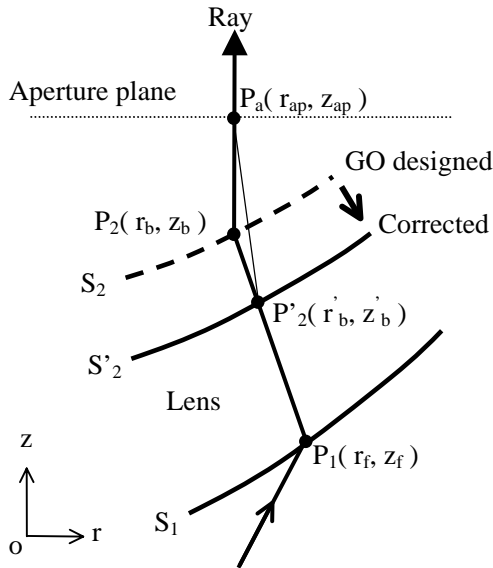


Fig.5 Phase correction by lens shaping

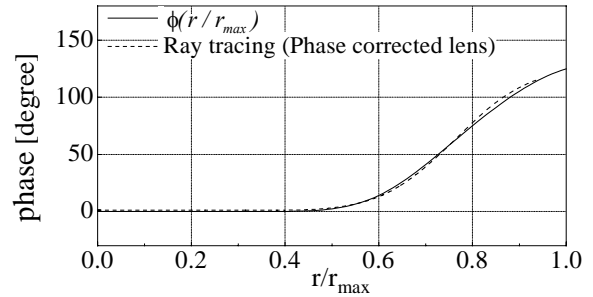


Fig.6 Traced aperture phase distribution

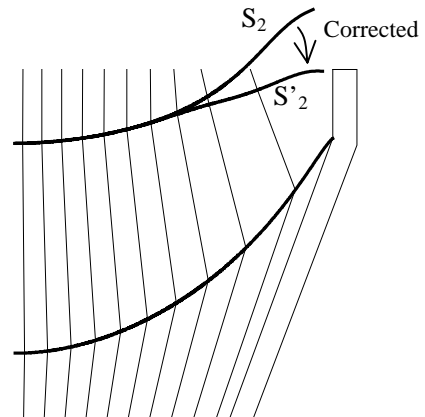


Fig.7 A corrected lens surface and traced ray

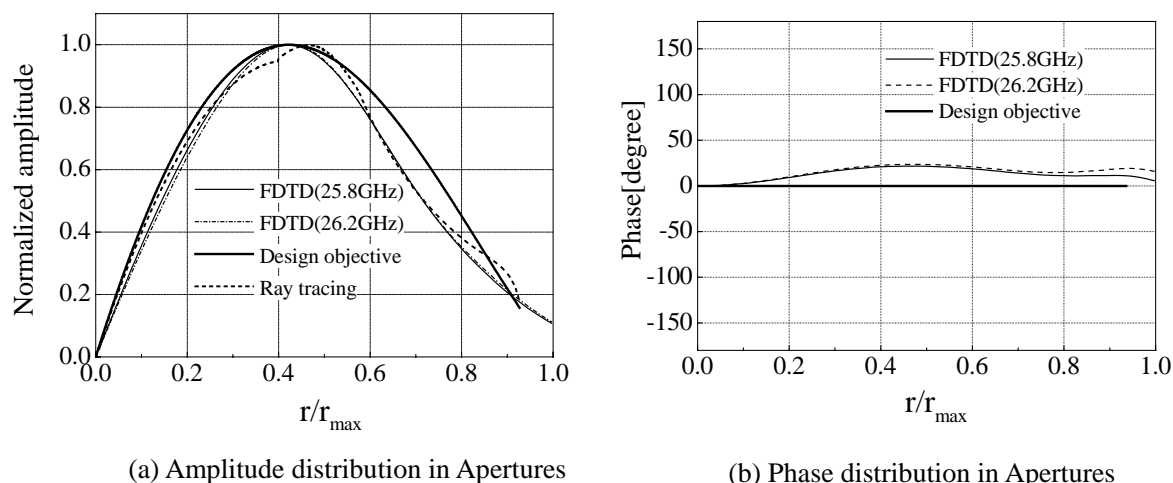


Fig.8 Aperture distributions of phase corrected dielectric lens

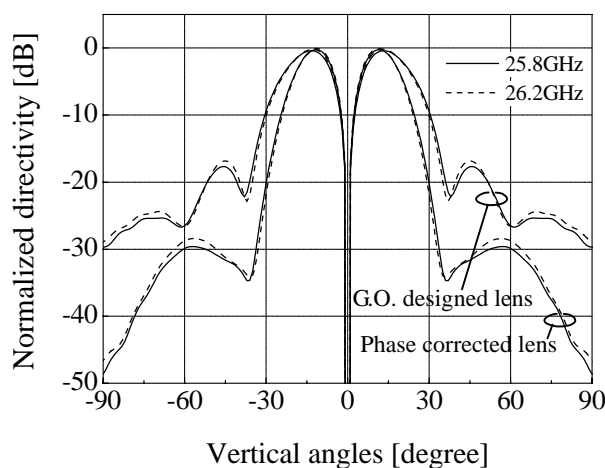


Fig.9 Radiation patterns through FDTD (Phase corrected lens)

5. Conclusion

Realizations of low sidelobe characteristics in a TM₀₁ dielectric lens horn are examined through FDTD analyses. In the case of an original geometrical optics design, phase delay of more than 100 degrees is occurred at the horn edge. Therefore, sidelobe levels become very high. The geometrical correction method is applied to the dielectric lens. Consequently, phase distributions become uniform. And sidelobe levels decrease more than 10 dB. Validity of a correction method is conceived. Sufficient low sidelobe levels (-30dB) in TM₀₁ mode dielectric lens horn is achieved.

REFERENCE

- [1] J.R.Bergmann, Flavio J. V. Hasselmann, and Marcos G.C. Branco, "A Single-Reflector Design for Omnidirectional Coverage", *Microwave Opt. Technol. Lett.*, vol.24, pp.426-429, March 2000
- [2] Atsushi Kezuka, Yasuhiro Kazama, Yoshihide Yamada, "Antennas with Coscant Squared Radiation Pattern Both Upward and Downward for FWA", *IEEE AP-S*, vol.2, pp.782-785, 2003
- [3] M. S. Narasimhan, M. Tech., and B. V. Rao, "Mode in a conical horn: new approach", *Proc. IEE*, Vol.118, No.2, Feb. 1971
- [4] A. D. Olver, P. J. B. Clarricoats, A. A. Kishk and L. Shafai, "Microwave Horn and Feeds", IEEE Press, 1994
- [5] William H. Press et al, "Numerical Recipes in FORTRAN, The Art of Scientific Computing Second Edition", Cambridge University Press, 1986